CrystEngComm

Accepted Manuscript

ROYAL SOCIETY OF CHEMISTRY

www.rsc.org/crystengcomm

Cite this: DOI: 10.1039/c0xx00000x

www.rsc.org/xxxxxx

ARTICLE TYPE

Chiral or achiral: Four Isomeric Cd(II) Coordination Polymers Based on Two Isomeric Phenylenediacrylate ligands †

Qian Sun, Ai-Ling Cheng, Kun Wang, Xiu-Chun Yi, En-Qing Gao *

Received (in XXX, XXX) Xth XXXXXXXXX 20XX, Accepted Xth XXXXXXXXX 20XX

DOI: 10.1039/b000000x

Four isomeric coordination polymers of formula $[Cd(L)(H_2O)_2]_n$ (L = ppda and mpda) were synthesized from two isomeric dicarboxylic ligands, *p*-phenylenediacrylic acid (H_2ppda) and *m*-phenylenediacrylic acid (H_2mpda). With the linear ppda ligand, compounds **1p** and **2p** crystallizes in centrosymmetric space groups, whereas the V-shaped mpda ligand induces spontaneous resolution to generate chiral crystals of **1m** and **2m** crystallized in chiral groups. Compounds **1p** and **1m** contain zigzag and helical $[Cd(L)]_n$ coordination chains, respectively, and show almost identical 2D chiral hydrogen-bonded networks formed via O-H···O interactions between $[Cd(COO)_2(H_2O)_2]$ units. In **1p** the centrosymmetric ppda ligand dictates an achiral 3D lattice. In **1m**, however, the acentric mpda linker and the hydrogen bonds collaborate to give a homochiral 3D network. Compounds **2p** and **2m** are both 3D coordination frameworks, built of similar μ-$O_{carboxylate}$ bridged helical chains and reinforced by similar 2D hydrogen-bonded networks. Ppda interlinks the helical chains in **2p** in a heterochiral fashion while mpda serves as chiral discriminative linkers between the chains in **2m** to give a 3D homochiral network. These compounds show enhanced ligand-centered luminescence.

1 Introduction

Chirality is a fascinating and fundamentally important phenomenon in nature and is an evergreen topic in many fields of science including biology, medicine, chemistry and materials science. The rapid development of coordination polymers, including metal-organic frameworks, opens new perspectives for the creation of new chiral solids for potential applications in asymmetric catalysis, chiral separation, biotechnology, and functional materials related to nonlinear optics, ferroelectrics, etc.[1-5] Thus far four general approaches toward chiral coordination polymers are known. The most straightforward approach uses an enantiopure precursor which comes into the final compound as a primary building block of the framework,[6-13] as an auxiliary ligand,[14-16] or occasionally as a templating guest.[17] The formation of the homochiral solid involves chiral conservation by which the chirality of the precursor is transferred to the whole solid. The second approach uses an enantiopure agent (solvent or additive) that induces chirality but does not get incorporated in the product,[18-21] but it is a difficult challenge to judiciously select a suitable agent for chiral induction. The third approach involves postsynthetic modification (PSM) of an achiral porous framework with an enantiopure agent,[22-24] and this is limited by the stability and reactivity of the mother frameworks. The above approaches all require the use of enantiopure agents, which are of limited availability and usually of high cost, and sometimes suffer from racemization. The fourth approach is to utilize spontaneous resolution,[25-38] a process that achiral or racemic building blocks assemble and crystallize into chiral crystals in absence of any enantiopure agent. Spontaneous resolution generally leads to conglomerates (racemic mixtures of enantiopure crystals). Products with an enantiomeric bias may occasionally be obtained because of statistical fluctuation of initial nucleation events,[29] and it may be possible to control the handedness through seeding.[39] Spontaneous resolution of chiral coordination polymers is determined by various factors such as ligand conformation and flexibility, metal coordination number and geometry, and supramolecular interactions such as hydrogen bonds and π-π stacking interactions. The process is unpredictable, but the probability of occurrence can be increased by, for example, choosing some ligands that tend to connect metal ions in twisted conformations to give chiral motifs. A nice example is the Mn(II) coordination polymers with 2-pyridylmethylketazine and azide, where the bis(chelating) diazine ligands are twisted upon complexation and the resulting chiral motifs are linked by asymmetric azide bridges.[40, 41] V-shaped organic bridging ligands with flexible tethers or coordinative groups (e.g., carboxylates) may lead to helical chain motifs, which can spontaneously resolve into 3D chiral structures provided that there are interchain homochiral interactions (coordination, hydrogen bonding and/or π-π stacking).[42-49]

Compared with the benzenedicarboxylic acids, which have been widely used for the construction of coordination polymers, phenylenediacrylic acids (Scheme 1) have two additional C=C bonds, which maintain the rigidity through the extended conjugation and meanwhile generate new features such as much expanded space between carboxylate groups and reduced steric hindrance around individual carboxylate groups. Among the

isomers, *p*-phenylenediacrylic acid (H_2ppda) has been used to construct a number of coordination polymers,[50-58] but the study of coordination polymers with *m*-phenylenediacrylic acid (H_2mpda) is still very limited.[59, 60] Our previous work have demonstrated that some Zn(II) and Mn(II) coordination polymers with the V-shaped mpda ligand display helical features but no spontaneous resolution occurred for lack of homochiral interactions between the helical motifs.[57, 58] In this article, we report four isomeric Cd(II) compounds derived from H_2mpda and H_2ppda. These compounds are of the same formula $[Cd(C_{12}H_8O_4)(H_2O)_2]_n$ ($C_{12}H_8O_4$ = ppda for **1p** and **2p,** and mpda for **1m** and **2m**), and structurally they fall into two pairs (**1p** and **1m**; **2p** and **2m**). **1p** and **1m** contain almost identical chiral hydrogen-bonded layers (each individual layer is homochiral), which are built of chiral $[Cd(COO)_2(H_2O)_2]$ units and linked into 3D hydrogen-bonded networks by dicarboxylate ligands. **2p** and **2m** contain almost identical μ-$O_{carboxylate}$ bridged helical chains, which are crosslinked into 3D coordination frameworks by dicarboxylate ligands. Despite the similarity of chiral motifs ($[Cd(COO)_2(H_2O)_2]$ units, chiral hydrogen-bonded layers or μ-O bridged helical chains) for each pair, spontaneous resolution occurs only for the mpda compounds (**1m** and **2m**), in which the V-shaped ligand selectively connects the chiral motifs of the same handedness to render homochirality to individual crystals. Differently, the linear ppda ligand acts as centrosymmetric connection to generate heterochiral 3D networks. The factors inducing the spontaneous resolution were discussed. In addition, the luminescent properties of these compounds were investigated.

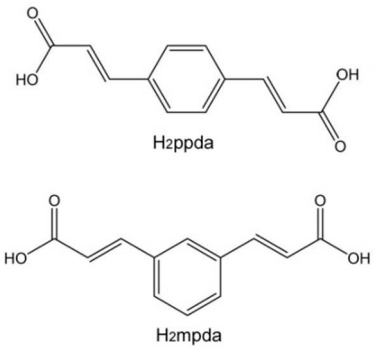

Scheme 1. Structures of the phenylenediacrylic acids used.

2 Experimental

2.1 Materials and general methods

All the reagents (purity ≥ 98 wt%) for synthesis were commercially available from Sinopharm Chemical Reagent Company (SCRC) and used without further purification.H_2ppda and H_2mpda were synthesized by literature methods,[61] Na_2ppda and Na_2mpda were prepared by adding ethanol to the aqueous solutions of the corresponding phenylenediacrylic acid and sodium hydroxide. Elemental analyses were carried out on an Elementar Vario ELIII analyzer. The FT-IR spectra (Fig. S1 in the ESI) were recorded in the range 400-4000 cm^{-1} using KBr pellets on a Nicolet NEXUS 670 spectrophotometer. Thermogravimetric analyses (TGA) were performed on a Mettler Toledo TGA/SDTA851 instrument under flowing air at a heating rate of 10°C min^{-1}. Powder X-ray diffraction data were collected on a Bruker D8–ADVANCE diffractometer equipped with Cu $K\alpha$ at a scan speed of 1° min^{-1}. Fluorescence spectra were recorded at room temperature on a Hitachi F-4500 Fluorescence Spectrophotometer.

2.2 Synthesis

Compound 1p. This compound was synthesized by a three-layer diffusion method. Above the aqueous solution (5 ml) of Na_2ppda (0.10 mmol, 0.026 g) in a 25 mL clean tube, a mixture of ethanol and water in the volume ratio of 1:1 and an ethanol solution of $Cd(OAc)_2{\cdot}6H_2O$ (0.10 mmol, 0.034 g) were successively dropped in with care to give a three-layer system, which was sealed and left undisturbed at room temperature for 2 weeks. Slow diffusion yielded colourless block crystals of **1p** and uncharacterized powders. The powders were removed by repeated decantation to give pure crystals in a yield of 0.021 g (56%). Elemental analysis (%) calc. for $C_{12}H_{12}CdO_6$: C 39.5, H 3.3; found: C 39.0, H 3.7. IR (KBr, cm^{-1}): 3210s, 3028s, 1638s, 1533s, 1506s, 1425vs, 1390vs, 1298w, 1262m, 1195w, 1112w, 979s, 880w, 830s, 731s, 622m, 504m.

Compound 2p. Crystals of **2p** were grown by a diffusion method similar to that for **1p** with some modification. Above the aqueous solution (5 ml) of Na_2ppda (0.10 mmol, 0.026 g) and bpea (0.10 mmol, 0.018 g) in a 25 mL clean tube, a mixture of ethanol and water in the volume ratio of 1:1 and an ethanol solution of $Cd(NO_3)_2{\cdot}6H_2O$ (0.1 mmol, 0.034 g) were successively dropped in to give a three-layer system, which was sealed and left undisturbed at room temperature for two weeks. Colourless rhombus crystals of **2p** appeared on the wall of the tube, concomitant with some pale precipitate at the bottom of the tube. The crystals were separated manually in yield 35%. Element analysis (%) calc. for $C_{12}H_{12}CdO_6$: C 39.5, H 3.3; found C 39.0, H 3.6. IR (KBr, cm^{-1}): 3400-3100br, 1668s, 1639s, 1550s, 1510s, 1420s, 1390vs, 1354sh, 1245m, 1143w, 1094w, 977s, 844s, 724s, 638w, 508w.

Compound 1m. A mixture of $Cd(NO_3)_2{\cdot}6H_2O$ (0.10 mmol, 0.034 g), H_2mpda (0.10 mmol, 0.022 g) and 1,2-bis(4-pyridyl)ethane (bpea, 0.10 mmol, 0.018 g) in DMSO (3 ml), DMF (2 mL) and water (1 mL) was stirred for 30 min in air, and then sealed and heated in a 23 mL Teflon-lined autoclave at 110 °C for 5 days. After cooling to room temperature slowly, yellow prism crystals of **1m** were obtained in a yield of 0.0115g (36%). Element analysis (%) calc. for $C_{12}H_{12}CdO_6$: C 39.5, H 3.3; found: C 40.0, H 3.1. IR (KBr, cm^{-1}): 3320m, 3196m, 3036m, 2919m, 2854w, 1642s, 1609s, 1560vs, 1430s, 1390vs, 1290w, 1223m, 1162w, 1070w, 1015m, 971m, 870w, 829m, 798m, 746w, 714w, 674w, 582m, 543m.

Compound 2m. A similar procedure to that for **1p** was followed to prepare crystals of **2m** except that Na_2ppda was replaced by Na_2mpda (0.1 mmol, 0.026g). Colorless block crystals of **2m** in yield 45% were obtained. Element analysis (%) calc. for $C_{12}H_{12}CdO_6$: C 39.5, H 3.3; found: C 39.0, H 3.5. IR (KBr, cm^{-1}): 3370s, 3222sh, 3030sh, 2925sh, 2854sh, 1640s, 1516vs, 1440s, 1398vs, 1298m, 1273m, 1240m, 1165m, 1093w, 977s, 874m, 822w, 798m, 760m, 678m, 592m, 542w.

Table 1 Crystal data and structure refinement for the compounds

Compound	**1p**	**1m**	**2p**	**2m**
Formula	$C_{12}H_{12}CdO_6$	$C_{12}H_{12}CdO_6$	$C_{12}H_{12}CdO_6$	$C_{12}H_{12}CdO_6$
M_r	364.62	364.62	364.62	364.62
Crystal system	monoclinic	Orthorhombic	monoclinic	Monoclinic
Space group	*C2/c*	$C222_1$	$P2_1/c$	$P2_1$
a/Å	11.823(2)	5.3146(8)	11.6229(4)	11.289(2)
b/Å	5.335(1)	11.977(2)	8.0177(3)	8.030(1)
c/Å	20.053(4)	19.719(3)	26.874(1)	14.209(4)
β/°	94.810(3)	90	93.789(1)	105.506(3)
V/Å^3	1260.4(5)	1255.2(3)	2498.9(2)	1262.1(5)
Z	4	4	8	4
D_c (g cm^{-3})	1.922	1.930	1.938	1.919
μ (mm^{-1})	1.752	1.759	1.767	1.750
Flack parameter	-	-0.01(5)	-	0.02(2)
Unique reflns	1436	1545	4899	5057
R_{int}	0.0336	0.0256	0.0286	0.0180
$R_1(I>2\sigma(I))$	0.0344	0.0181	0.0420	0.0266
wR_2(all data)	0.0808	0.0472	0.0972	0.0628

2.3 Crystal datas collection and refinement:

X-ray Crystallographic Measurements. A summary of the crystallographic data, data collection, and refinement parameters for the complexes are provided in Table 1 with selected distances and angles of the structures listed in Table 2. Diffraction data for these compounds were collected at ambient temperature on a Bruker Apex II CCD area detector equipped with graphite-monochromated Mo Kα radiation (λ = 0.71073 Å). Empirical absorption corrections were applied using the SADABS program.[62] The structures were solved by the direct method and refined by the full-matrix least-squares method on F^2, with all non-hydrogen atoms refined with anisotropic displacement parameters.[63] The hydrogens attached to carbons were placed in calculated positions and refined using the riding model, and the water hydrogens were located from the difference maps and refined with isotropic displacement parameters and with distance and angle restraints. A centroymmetric ppda ligand in **2p** displays disorder over two independent components (C19 – C24, O9 and O10; C19' – C24', O9' and O10') with refined occupancies of 0.57 and 0.43. Another ppda ligand displays partial disorder in the phenylene ring and one acrylate group (C4 – C12, O3 and O4; C4' – C12', O3' and O4'), the occupancies of the two components being refined to be 0.47 and 0.53. To get better anisotropic and geometric parameters for the phenylene rings, SHELXL DELU and SADI restraints [63] were applied in the final refinements. A diagram showing the disorder of the ligands is given in Fig. S1 in the ESI.

3 Results and discussion

3.1 Synthesis and general characterization

Among the complexes reported in this article, compound **1m** was prepared from H_2mpda under solvothermal conditions while the other compounds were synthesized from Na_2mpda or Na_2ppda by liquid diffusion methods. Compounds **1p** and **2m** were obtained under similar conditions in the absence of additives. **1p** was also prepared elsewhere from the hydrothermal reaction of H_2ppda and $CdCl_2$ in the presence of NaOH.[64] It is noteworthy that compounds **1m** and **2p** were synthesized in the presence of bpea, a ditopic N-donor ligand widely used for the construction of high-dimensional coordination polymers with mixed carboxylate and pyridyl ligands. The fact that bpea did not appear in compounds **1m** and **2p** impelled us to investigate whether the compounds can be obtained in the absence of the bpea under otherwise identical conditions. It turned out that the reaction of H_2mpda with $Cd(NO_3)_2$ in the absence of bpea under the conditions for preparing **1m** yielded a yellow powder that is different from **1m** according to X-ray diffraction. The reaction of Na_2ppda (Na_2mpda) with $Cd(NO_3)_2$ in the absence of bpea under the conditions for preparing **2p** yielded compound **1p** (**2m**). isolated Obviously, the bis(bipyridyl) ligand plays a kind of structure-directing role in the formation of compounds **1m** and **2p**, though the detailed mechanism is unclear.

The experimental powder X-ray diffraction patterns (Fig. S2 in the ESI) of the bulk samples are in agreement with those simulated using crystallographic data. The FT-IR spectra of these compounds (Fig. S3 in the ESI) are similar and show no absorption bands around 1700 cm^{-1}, consistent with the complete deprotonation of the carboxylic groups of the organic ligand in the compounds. The strong absorption in the range of 1638-1640cm^{-1} may be assigned to the υ_{as}(COO) vibration, and the strong bands at about 1390 cm^{-1} to υ_s(COO). All the compounds show bands in the region 3300-3400cm^{-1}, which can be assigned to water molecules.

3.2 Descriptions of crystal structures

The four compounds are structural isomers with the same formula of $[Cd(C_{12}H_8O_4)(H_2O)_2]_n$. **1p** and **2p** are isomeric with **1m** and **2m** because of the *p* and *m* position isomerism of the phenylenediacrylate ligands. Each ligand leads to two coordination isomers (or supramolecular isomers) different in metal-ligand coordination modes and networks. The two isomers derived from ppda (**1p** and **2p**) crystallized in different centrosymmetric space groups, while those derived from mpda (**1m** and **2m**) crystallized in chiral groups. Despite the difference in symmetry, **1p** and **1m** bear some resemblances in coordination and hydrogen bonding networks, and so do **2p** and **2m**. The structure of **1p** has been reported elsewhere very briefly.[64] Here we describe and compare the structures as follows.

Compounds 1p and **1m.** Single-crystal X-ray diffraction revealed that compounds **1p** and **1m** are 1D coordination polymers (Figure 1). The asymmetric units of the two structures are similar, each containing half an Cd(II) ion, half a dicarboxylate anion (ppda or mpda), and a coordinated water molecule. The coordination geometry around Cd(II) is almost identical in the two compounds, with very minor differences in structural parameters. In each compound, the Cd(II) ion is located on a 2-fold axis (along the *b* (**1p**) or *a* (**1m**) direction) and coordinated by six oxygen atoms from two chelating carboxylic groups (O1, O2 and O1A, O2A, with Cd-O = 2.31-2.38 Å) and two water molecules (O3 and O3A, with Cd-O = 2.21 Å). The small O-Cd-O bite angles of the chelating carboxylate groups (55.43(8)º for **1p** and 55.57(5)º for **1m**) cause severe distortion of the coordination geometry from octahedral. The geometry may be better described as a distorted trigonal prism, for which each basal face is defined by three non-equivalent oxygens, with two water oxygens defining a long lateral edge and each chelating carboxylate group defining a short lateral edge.

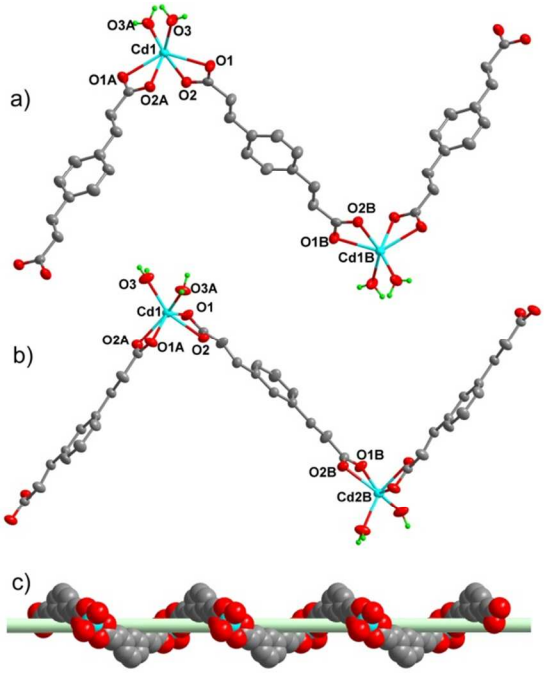

Figure 1. Coordination environments and chain structures in **1p** (a) and **1m** (b), ellipsoids drawn at the 30% probability level. The helical chain in **1m** is highlighted in c), where the pale green rod represents the virtual helical axis. Symmetry codes: A = -*x*+1, *y*, -*z*+3/2; B = -*x*+1/2, -*y*+5/2, -*z*+1 for **1p**; A = *x*, -*y*+2, -*z*; B = -*x*, *y*, -*z*+1/2 for **1m**.

The ppda or mpda ligands serve as bis(chelating) ditopic bridges to link Cd(II) ions into infinite coordination chains, with Cd…Cd = 15.75 Å for **1p** and 14.53 Å for **1m**. Despite the almost identical local coordination environments around Cd in **1p** and **1m**, the different geometry of ppda and mpda leads to different chain shapes. The ppda ligand is linear and lies about an inversion centre. The symmetry in combination with the cis-arrangement of the two carboxylate groups around Cd, dictates a zigzag chain with metal ions at corners (Figure 1a). The turning angle (defined by three adjacent metal ions) is 90.66° and the pitch is 22.41 Å. The zigzag chain is parallel to the (10-1) plane and propagates long the [101] direction. Differently, mpda has the centrosymmetry-incompatible bent shape and resides on a 2-fold axis along the *b* direction, which passes through the C5 and C7 atoms of the phenylene ring. A helical chain spiraling around the 2_1 screw axis is generated along the *c* direction (Figure 1b,c), with the pitch (19.719 Å) equal to the *c* dimension of the unit cell. Consistent with the chain shape and symmetry, the chain in **1p** is heterochiral because adjacent $[Cd(COO)_2(H_2O)_2]$ moieties exhibit opposite handedness while the chain in **1m** is homochiral with all Cd centers in it having the same handedness.

The chains in **1p** and **1m** are closely packed in parallel with interchain O-H···O hydrogen bonds involving all water hydrogen atoms and all carboxylate oxygens. Despite the different chain shapes, the hydrogen bonding networks in **1p** and **1m** are very similar. Each coordinated water molecule (O3) around a Cd ion donates its hydrogen atoms to two carboxylate oxygen atoms (O1C and O2D) coordinated to two different Cd(II) ions (Figure 2, the relevant parameters are listed in Table S1). Two equivalent O3-H···O2 hydrogen bonds (related by the 2-fold axis along the *b* (**1p**) or *a* (**1m**) direction) serve as crossed spiral bridges between neighboring Cd(II) ions, with the Cd-O-O-Cd torsion angle being 91.2º (**1p**) or 93.3º (**1m**). This leads to a double-strand helicate-like dinuclar $[M(OH…O)_2M]$ unit, with the Cd…Cd distance equal to the *b* (**1p**) or *a* (**1m**) dimension of the cell. The helicate unit repeats translationally to give doubly hydrogen-bonded chains along the *b* (**1p**) or *a* (**1m**) direction, and the O3-H···O1 hydrogen bonds further connect translation-related chains to generate a 2D hydrogen-bonded layer along the *ab* plane. Obviously, in both **1p** and **1m**, all $[Cd(COO)_2(H_2O)_2]$ moieties connected by hydrogen bonds have the same handedness, that is, each hydrogen-bonded layer is homochiral. In the layer, each Cd(II) ion is linked to six neighbors through the hydrogen bonds, and taking Cd(II) as node and hydrogen bonds as links, the layer can be simplified into a 2D (3,6) triangular net (point symbol $3^6.4^6.5^3$).

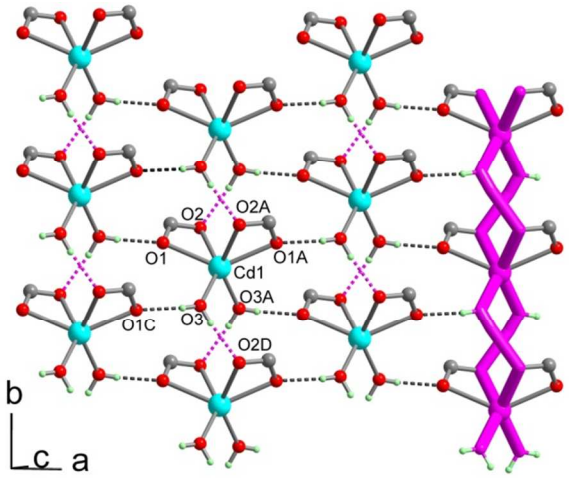

Figure 2. A homochiral 2D hydrogen-bonded layer in **1p**. The layer in **1m** is almost identical (the same atom-labeling scheme is used). A chain containing the helicate-like $[M(OH…O)_2M]$ dinuclear moietiy is highlighted with thick bonds. Symmetry codes: C = -*x*+1/2, *y*-1/2, -*z*+3/2; D = -*x*+1, *y*-1, -*z*+3/2 for **1p**; C = *x*+1/2, -*y*+3/2, -*z*; D = *x*+1, -*y*+2, -*z* for **1m**.

Taking into account both the hydrogen bonds and the dicarboxylate linkers, it is convenient to view the whole

structures of **1p** and **1m** as 3D pillared-layer architectures in which hydrogen bonded layers are pillared by covalent linkers (Figure 3, left). A close inspection reveals that that each chain is connected to six others via hydrogen bonds (Figure 3, right). The zigzag chains in **1p** are arranged in an interdigitating manner into layers parallel to the (10-1) plane, and the helical chains in **1m** are entangled with one another (Figure S4). Topologically, the underlying nets of the two structures are the same, resulting from the simple node-to-node connection of the 2D triangular nets and belonging to the **hex** 3D net (point symbol $3^6.4^{18}.5^3.6$). Despite the same chiral hydrogen-bonded layer and the same 3D net topology for the two compounds, the centrosymmetric ppda linkers dictates opposite handedness in **1p**, whereas the C_2-symmetric V-shaped mpda linkers in **1m** serve as "homochiral" connections between chiral Cd(II) centers and chiral layers. Therefore, compound **1p** crystallizes in a centrosymmetric space group (*C2/c*), while **1m** crystallizes with spontaneous resolution in a chiral group ($C222_1$). Compounds **1p** and **1m** represent an example of identical chiral motifs ($[Cd(COO)_2(H_2O)_2]$ moiety and homochiral hydrogen-bonded layer) being assembled into hetero- and homochiral 3D networks through linear and V-shaped isomeric ligands, respectively.

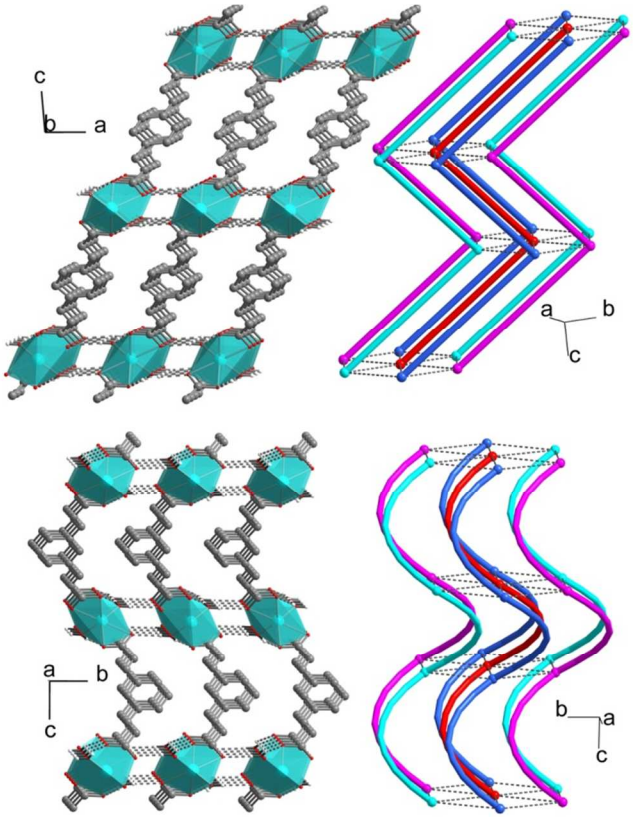

Figure 3. Diagrams showing the 3D hydrogen-bonded networks and schematic illustrations showing the arrangement of chains (The dotted lines represent the hydrogen bonding connections between the chains) (top: **1p**, bottom: **1m**).

The comparison between **1p** and **1m** obviously suggests that the geometry of the mpda linker, which connects metal ions into helical chains or serves as homochiral connections between chiral layers, is crucial in inducing spontaneous resolution. However, equally crucial are the O-H···O hydrogen bonding interactions, via which the chiral $[Cd(COO)_2(H_2O)_2]$ moieties (and the helical chains) are assembled in a homochiral manner. In a previous Zn(II) compound with mpda ([Zn(mpda)(phen)] with phen =1,10-phenanthroline, which is in the chelating mode and replaces the water ligands in **1m**),[57] chiral metal centers are also linked into helical chains by bis(chelating) mpda ligands, as found in **1m**. However, in the absence of O-H···O hydrogen bonds, the chiral $[Zn(COO)_2(phen)]$ moieties and the helical chains in [Zn(mpda)(phen)] are assembled in a heterochiral manner through the π-π interactions that involve centrosymmetry-related phen ligands. Therefore, the spontaneous resolution observed for **1m** arises from two collaborative crucial ingredients—the acentric mpda linker and the extended hydrogen bonding interactions: the mpda linker provides homochiral coordinative connections in one dimension, while the hydrogen bonding network provides homochiral supramolecular interactions in the other two dimensions. [Zn(mpda)(phen)] and **1p** represent the cases with only the coordinative linker and with only the hydrogen bonds, respectively, where the homochirality is limited to only one or two dimensions.

Compounds 2p and 2m. These two compounds represent another example of identical chiral motifs being assembled into hetero- and homochiral 3D networks through isomeric ppda and mpda linkers, respectively, but different from the 3D hydrogen-bonded networks of **1p** and **1m**, here 3D coordination networks are formed.

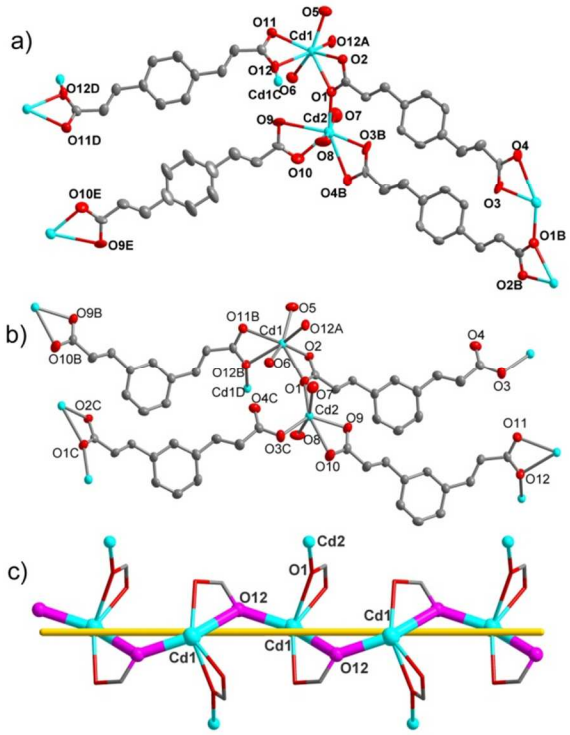

Figure 4. Coordination environments of Cd(II) and the ligands in **2p** (a) and **2m** (b); the helical $[Cd\text{-}O]_n$ chain present in both compounds is illustrated in c), where the yellow rod represents the helical axis. Symmetry codes for **2p**: A: *-x*+1, *y*-1/2, *-z*+1/2; B: *-x*+2, *-y*+1, *-z*; C: *-x*+1, *y*+1/2, *-z*+1/2; D: *-x*+1, *-y*+1, *-z*+1; E: *-x*+2, *-y*+1, *-z*+1; for **2m**: A: *-x*+1, *y*-1/2, *-z*+1; B: *x*+1, *y*, *z*+1; C: *x*, *y*, *z*+1; D, 2-*x*, 0.5+*y*, 2-*z*. The disorder of some ligands in **2p** is not shown here but in Fig. S3 in the ESI.

2p crystallizes in the centrosymmetric $P2_1/c$ space group, and

2m in the chiral $P2_1$ group. Both structures contain two independent Cd(II) ions (Figure 4). Cd1 are seven-coordinated by two chelating carboxylate groups, two water molecules and an oxygen atom from a carboxylate chelating an adjacent Cd1, with the Cd1-O distances in the range of 2.29-2.46 Å. The coordination leads to a distorted pentagonal bipyramidal geometry, for which the axis is defined by two 2_1-related carboxylate oxygens. Cd2 is six-coordinated by a chelating carboxylate group, two *trans*-positioned water molecules and two additional oxygen atoms from different carboxylate groups, resulting in a highly distorted octahedral geometry. The geometrical distortion arises from the small O-Cd-O bite angle (51.8-54.7°) of the chelating carboxylate groups and the widely varied Cd-O bond distances (2.20-2.75 Å). Cd1 and Cd2 are connected into a dinuclar unit by a single μ-O atom (O1) that arises from the carboxylate group chelating Cd1, with Cd1…Cd2 = 4.4182(6) Å (**2p**) or 4.4695(8) Å (**2m**). Furthermore, adjacent Cd1 atoms related by the 2_1 axis are connected by single μ-O bridges (O12) that arise from another set of carboxylates, with Cd1…Cd1 = 4.1552(6) Å (**2p**) or 4.1504(6) Å (**2m**). This leads to an infinite 1D helical $[Cd1\text{-}O12]_n$ chain along the *b* direction (Figure 4c), the pitch being equal to the *b* dimension of the unit cell. The Cd1-O1-Cd2 moieties serve as side arms alternately stretching out from opposite sides of the chain.

The helical chains in **2p** and **2m** are connected into 3D networks in different manners by different dicarboxylate ligands. In **2p**, there are three independent ligands assuming different coordination modes (Figure 4a), two of which show disorder over two sites in whole or in part (Fig. S1 in the ESI). The ligand with O11 and O12 serves as a centrosymmetric bis(chelating-bridging) μ_4 linker, with each carboxylate group chelating a Cd1 and binding another Cd1 through μ-O12. The disordered ligand with O9/O9' and O10/O10') is also centrosymmetric and serves as a bis(chelating) μ_2 linker, with each carboxylate group chelating a Cd2 atom. The partially disordered ligand with O1, O2, O3/O3' and O4/O4') is an asymmetric μ_3 linker, with a chelating-bridging carboxylate group (chelating Cd1 and binding Cd2 through μ-O1) and a monodentate carboxylate (binding another Cd2). The asymmetric ligands appear in pairs and each pair serve as centrosymmetric double linkers between chains. Through above centrosymmetric single and double linkers, each helical chain in **2p** is connected with six others to produce a complicated 3D framework. It is evident that the helical chains connected by the linkers have opposite handedness, that is, the framework is heterochiral.

In **2m**, there are two independent mpda ligands in different μ_3 bridging modes (Figure 4b), both being asymmetric. One is similar to the μ_3-ppda linker in **2p** and has a chelating-bridging carboxylate (binding Cd1 and Cd2) and a monodentate carboxylate (binding another Cd2); The other mpda ligand has a chelating-bridging carboxylate (binding two Cd1 atoms) and a chelating carboxylate (binding Cd2). Through these asymmetric linkers, each helical chain in **2m** is connected with four others with the same handedness to produce a 3D homochiral framework.

Topological analysis was carried out to better understand the complicated 3D frameworks of **2p** and **2m**. For this purpose, a reasonable approach is to reduce the Cd1-Cd2 dinuclear units (4- and 5- connected in **2p** and **2m**, respectively) and the carboxylate groups (or the O12 atoms, 3-connected) between Cd1 atoms into nodes, and meanwhile the Cd1-O12 bonds and the organic bridging ligands are taken as links. Thus, the 3D frameworks of **2p** and **2m** are reduced to 3,4- and 3,5-connected binodal nets (Figure 5), respectively, with point symbols $(8^3)(8^6)$ and $(6^3)(6^9.8)$, respectively, according to TOPOS calculations (the RCSR three-letter symbol [65] for the latter net is **hms**).[66] The hetero- or homochirality of **2p** or **2m**, respectively, is evident from the handedness of the helical chains in the net diagrams shown in Figure 5. The net of **2p** represents a new net topology not yet recognized prior to this study. It has only eight-numbered shortest cycles around each node and features self-catenation between relatively inclined cycles.

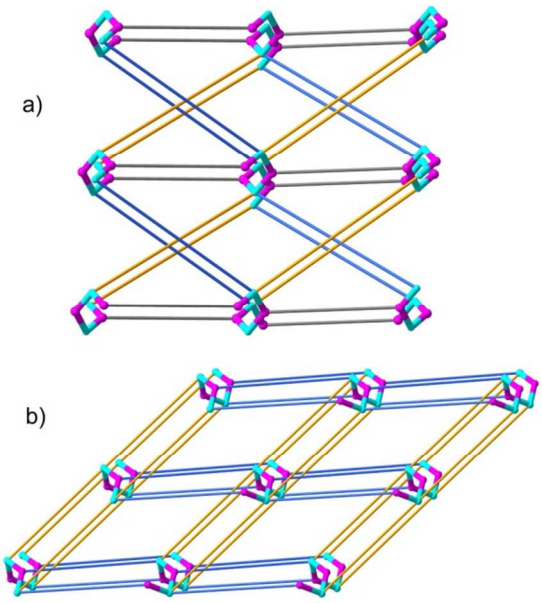

Figure 5. Simplified 3D nets for the coordination networks in **2p** (a) and **2m** (b). The $[Cd1\text{-}O12]_n$ helical chains are highlighted by thick rods. The hetero- or homochirality is evident from the handedness of the helical chains.

In both **2p** and **2m**, the coordinated water molecules and the carboxylate oxygen atoms form plenty of intrachain and interchain O-H…O hydrogen bonds (Figure S5. The relevant parameters are listed in Table S1). The intrachain hydrogen bonds help to reinforce the helical chains and the interchain ones make the chains interdigitate like zippers to give a 2D layer along the *ab* plane. Each hydrogen-bonded layer in **2p** and **2m** is homochiral. In this sense, the formation of the homo- and heterochiral 3D networks in **2p** and **2m**, respectively**,** is similar to that in **1p** and **1m**. In **1p** and **2p**, the ppda ligands interlink hydrogen-bonded layers of opposite chirality, while the mpda ligands in **1m** and **2m** selectively interlink layers with the same chirality. However, the differences between **1m** and **2m** are also evident. In **1m,** mpda is responsible for the chirality in one dimension by forming helical chains, and the chiral discrimination in the other two dimensions between the helical chains is completed by hydrogen bonds. In **2m**, however, 1D helicity is generated by $\mu\text{-}O_{carboxylate}$ bridges, and the chiral discrimination in the other two dimensions is completed by interchain mpda linkers. It may be said that the hydrogen bonds

in **1m** are primary forces to organize helical chains into a 3D structure in a homochiral fashion while those in **2m** serve as secondary forces to reinforce the helical chains and the 3D homochiral coordination framework.

3.3 Luminescent properties

The luminescent properties of the two free ligands and the coordination compounds were measured in the solid state at room temperature (Figure 6). The free ligand H_2ppda exhibits broad emission bands at 415 and 430 nm (λ_{ex} = 300 nm), which could be attributed to intraligand π^*-n or π^*-π transitions. Compound **2p** displays similar and somewhat stronger emission bands at 415 and 435 nm (λ_{ex}=360 nm), while compound **1p** exhibits very broad and much more intense emission around 450 nm with a shoulder at about 415 nm (excited at 380 nm). These compounds all shows evident low-energy trailing in the spectral profiles. Compared with the spectrum of the free ligand, the emission bands of the Cd(II) compounds can be attributed to the electronic transitions within the metal-modified ligand. The emission associated with charge transfer transitions between metal ions and ligands is unlikely owing to the poor electron accepting/donating ability of the mononuclear Cd(II) center. The enhancement of luminescent intensity in the complexes could be because the metal coordination increases the rigidity of the ligands and reduces the energy loss through radiationless decay. The effect is more significant for **1p**.

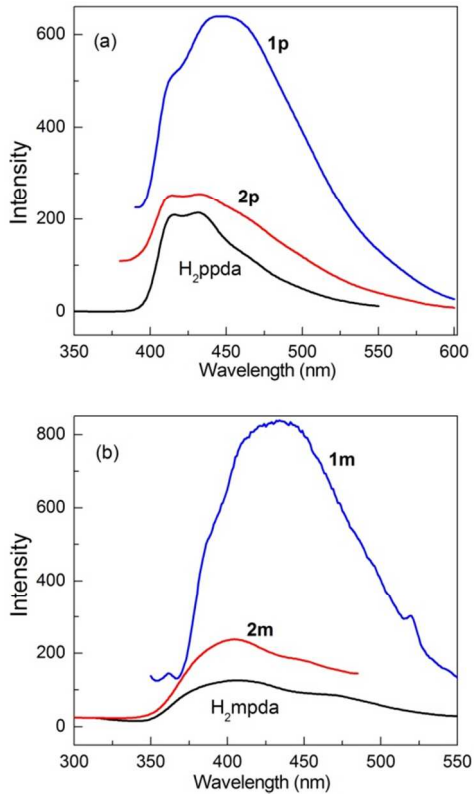

Figure 6 Solid-state photoluminescence spectra of (a) ligand H_2ppda and complexes **1p**, **2p**; and (b) ligand H_2mpda and complexes **1m**, **2m** at room temperature.

Similar effects were observed for H_2mpda, **1m** and **2m**. The ligand shows a very broad main emission band at about 405 nm with a trailing shoulder at about 460 nm (λ_{ex} = 295 nm). The spectrum of **2m** is very similar, showing a broad band at about 405 nm and a shoulder at about 445 nm. **1m** shows significantly increased fluorescence, with a broad band centered at 433 nm and a high-energy shoulder at about 390 nm.

4 Conclusions

We succeeded in isolating four isomeric coordination compounds of formula $[Cd(C_{12}H_8O_4)(H_2O)_2]_n$ with the isomeric ppda and mpda ligands. Compounds **1p** and **1m** contain almost identical hydrogen- bonded layers built of chiral $[Cd(COO)_2(H_2O)_2]$ units, and each layer is homochiral. In **1p**, ppda connects Cd(II) into centrosymmetric zigzag chains and thus connects the layers in a heterochiral manner to give an achiral 3D lattice. In **1m**, however, mpda connects Cd(II) into helical chains and thus connects the layers in a homochiral manner to give chiral crystals. The spontaneous resolution arises from the collaborative chiral discrimination through the V-shaped ligand and the extended hydrogen bonding networks. Compounds **2p** and **2m** are 3D coordination frameworks containing almost identical μ-$O_{carboxylate}$ bridged helical chains. Again, ppda as interchain linkers leads to an achiral 3D framework for **2p** while mpda serves as homochiral connectors between the helical chains to evoke spontaneous resolution for **2m**, with hydrogen bonding interactions being secondary forces to reinforce the framework. Spontaneous resolution of chiral coordination polymers is a multifactorial process, and it is still impossible, with our present state of knowledge, to predict its occurrence, but one can increase the probability of the occurrence by choice of building blocks. With this work, we have shown that isomeric V-shaped and linear ligands can lead to coordination polymers with similar coordination and hydrogen bonding networks, but only the V-shaped ligand generates chiral 3D networks, thus demonstrating the importance of ligand geometry in inducing spontaneous resolution.

Acknowledgements

This work is supported by the National Natural Science Foundation of China (Nos. 21103051 and 21173083) and the Research Fund for the Doctoral Program of Higher Education of China.

Notes and references

Shanghai Key Laboratory of Green Chemistry and Chemical Processes, Department of Chemistry, East China Normal University, Shanghai 200062, P. R. China.E-mail: eqgao@chem.ecnu.edu.cn; Fax: +86-21-62233404; Tel: +86-21-62233404.

†Electronic Supplementary Information (ESI) available: Hydrogen bonding parameters and additional structural diagrams. CCDC 969455-969456. For ESI and crystallographic data in CIF or other electronic format see DOI: 10.1039/XXXX.

1 M. Yoon, R. Srirambalaji and K. Kim, *Chem. Rev.*, 2012, **112**, 1196-1231.
2 X.-L. Yang and C.-D. Wu, *CrystEngComm*, 2014, **16**, 4907-4918.
3 Y. Liu, W. M. Xuan and Y. Cui, *Adv. Mater.*, 2010, **22**, 4112-4135.
4 L. Q. Ma, C. Abney and W. B. Lin, *Chem. Soc. Rev.*, 2009, **38**, 1248-1256.
5 W. Zhang, H.-Y. Ye and R.-G. Xiong, *Coord. Chem. Rev.*, 2009, **253**, 2980-2997.
6 W. Xuan, C. Ye, M. Zhang, Z. Chen and Y. Cui, *Chem. Sci.*, 2013, **4**, 3154-3159.

7 J. S. Seo, D. Whang, H. Lee, S. I. Jun, J. Oh, Y. J. Jeon and K. Kim, *Nature*, 2000, **404**, 982-986.
8 L. Ma, J. M. Falkowski, C. Abney and W. Lin, *Nat. Chem.*, 2010, **2**, 838-846.
9 F. J. Song, C. Wang, J. M. Falkowski, L. Q. Ma and W. B. Lin, *J. Am. Chem. Soc.*, 2010, **132**, 15390-15398.
10 Y. Peng, T. Gong, X. Lin, Y. Liu, Y. Cui, K. Zhang and J. Jiang, *Nat Commun*, 2014, **5**, 4406.
11 E. V. Anokhina, Y. B. Go, Y. Lee, T. Vogt and A. J. Jacobson, *J. Am. Chem. Soc.*, 2006, **128**, 9957-9962.
12 K. Mo, Y. Yang and Y. Cui, *J. Am. Chem. Soc.*, 2014, **136**, 1746-1749.
13 C. Zhu, X. Chen, Z. Yang, X. Du, Y. Liu and Y. Cui, *Chem. Commun.*, 2013, **49**, 7120-7122.
14 P. Wu, C. He, J. Wang, X. Peng, X. Li, Y. An and C. Duan, *J. Am. Chem. Soc.*, 2012, **134**, 14991-14999.
15 D. B. Dang, P. Y. Wu, C. He, Z. Xie and C. Y. Duan, *J. Am. Chem. Soc.*, 2010, **132**, 14321-14323.
16 D. Bradshaw, T. J. Prior, E. J. Cussen, J. B. Claridge and M. J. Rosseinsky, *J. Am. Chem. Soc.*, 2004, **126**, 6106-6114.
17 M. Gruselle, Y. Li, N. Ovanesyan, V. Makhaev, G. Shilov, F. Mushenok, C. Train and S. Aldoshin, *Chirality*, 2013, **25**, 444-448.
18 Y. Kang, S.-M. Chen, F. Wang, J. Zhang and X.-H. Bu, *Chem. Commun.*, 2011, **47**, 4950-4952.
19 R. E. Morris and X. Bu, *Nat Chem*, 2010, **2**, 353-361.
20 Y. Wen, T. Sheng, Z. Sun, Z. Xue, Y. Wang, Y. Wang, S. Hu, X. Ma and X. Wu, *Chem. Commun.*, 2014, **50**, 8320-8323.
21 X. Jing, C. He, D. Dong, L. Yang and C. Duan, *Angew. Chem. Int. Ed.*, 2012, **51**, 10127-10131.
22 J. Canivet, S. Aguado, G. Bergeret and D. Farrusseng, *Chem. Commun.*, 2011, **47**, 11650-11652.
23 W. Zhu, C. He, P. Wu, X. Wu and C. Duan, *Dalton Trans.*, 2012, **41**, 3072-3077.
24 M. Banerjee, S. Das, M. Yoon, H. J. Choi, M. H. Hyun, S. M. Park, G. Seo and K. Kim, *J. Am. Chem. Soc.*, 2009, **131**, 7524-7525.
25 R.-Q. Zou, R.-Q. Zhong, M. Du, D. S. Pandey and Q. Xu, *Cryst. Growth Des.*, 2008, **8**, 452-459.
26 X.-D. Chen, M. Du and T. C. W. Mak, *Chem. Commun.*, 2005, 4417-4419.
27 L. Perez-Garcia and D. B. Amabilino, *Chem. Soc. Rev.*, 2007, **36**, 941-967.
28 K. Biradha, C. Seward and M. J. Zaworotko, *Angew. Chem., Int. Ed.*, 1999, **38**, 492-495.
29 U. Siemeling, I. Scheppelmann, B. Neumann, A. Stammler, H.-G. Stammler and J. Frelek, *Chem. Commun.*, 2003, 2236-2237.
30 S. Chen, J. Zhang and X. Bu, *Inorg. Chem.*, 2009, **48**, 6356-6358.
31 B. Gil-Hernandez, H. A. Hoeppe, J. K. Vieth, J. Sanchiz and C. Janiak, *Chem. Commun.*, 2010, **46**, 8270-8272.
32 X.-L. Tong, T.-L. Hu, J.-P. Zhao, Y.-K. Wang, H. Zhang and X.-H. Bu, *Chem. Commun.*, 2010, **46**, 8543-8545.
33 J.-L. Liu, X. Bao, J.-D. Leng, Z.-J. Lin and M.-L. Tong, *Cryst. Growth Des.*, 2011, **11**, 2398-2403.
34 K. K. Bisht and E. Suresh, *J. Am. Chem. Soc.*, 2013, **135**, 15690-15693.
35 W. Liu, X. Bao, L.-L. Mao, J. Tucek, R. Zboril, J.-L. Liu, F.-S. Guo, Z.-P. Ni and M.-L. Tong, *Chem. Commun.*, 2014, **50**, 4059-4061.
36 S. Yuan, Y.-K. Deng, W.-M. Xuan, X.-P. Wang, S.-N. Wang, J.-M. Dou and D. Sun, *CrystEngComm*, 2014, **16**, 3829-3833.
37 L. Qin, J. S. Hu, M. D. Zhang, Z. J. Guo and H. G. Zheng, *Chem Commun (Camb)*, 2012, **48**, 10757-10759.
38 H.-X. Zhang, F. Wang, Y.-X. Tan, Y. Kang and J. Zhang, *J. Mater. Chem.*, 2012, **22**, 16288-16292.
39 T. Ezuhara, K. Endo and Y. Aoyama, *J. Am. Chem. Soc.*, 1999, **121**, 3279-3283.
40 E.-Q. Gao, S. Q. Bai, Z. M. Wang and C. H. Yan, *J. Am. Chem. Soc.*, 2003, **125**, 4984-4985.
41 E.-Q. Gao, Y.-F. Yue, S.-Q. Bai, Z. He and C.-H. Yan, *J. Am. Chem. Soc.*, 2004, **126**, 1419-1429.
42 X.-Y. Duan, Q.-J. Meng, Y. Su, Y.-Z. Li, C.-Y. Duan, X.-M. Ren and C.-S. Lu, *Chem. Eur. J.*, 2011, **17**, 9936-9943.
43 K. K. Bisht and E. Suresh, *Inorg. Chem.*, 2012, **51**, 9577-9579.
44 X. Tan, J. X. Zhan, J. Y. Zhang, L. Jiang, M. Pan and C. Y. Su, *CrystEngComm*, 2012, **14**, 63-66.
45 S. Ding, Y. Gao, Y. Ji, Y. Wang and Z. Liu, *CrystEngComm*, 2013, **15**, 5598-5601.
46 J.-W. Lin, P. Thanasekaran, J.-S. Chang, J.-Y. Wu, L.-L. Lai and K.-L. Lu, *CrystEngComm*, 2013, **15**, 9798-9810.
47 Q. Yang, L. Huang, M. Zhang, Y. Li, H. Zheng and Q. Lu, *Cryst. Growth Des.*, 2013, **13**, 440-445.
48 Z.-L. Zhang, X.-Q. Yao, N. An, H.-C. Ma, Z.-Q. Lei and J.-C. Liu, *Inorg. Chem. Commun.*, 2014, **45**, 127-130.
49 A. Goswami, S. Bala, P. Pachfule and R. Mondal, *Cryst. Growth Des.*, 2013, **13**, 5487-5498.
50 Q.-R. Fang, G.-S. Zhu, M. Xue, Q.-L. Zhang, J.-Y. Sun, X.-D. Guo, S.-L. Qiu, S.-T. Xu, P. Wang, D.-J. Wang and Y. Wei, *Chem. Eur. J.*, 2006, **12**, 3754-3758.
51 K.-L. Huang, X. Liu, J.-K. Li, Y.-W. Ding, X. Chen, M.-X. Zhang, X.-B. Xu and X.-J. Song, *Cryst. Growth Des.*, 2010, **10**, 1508-1515.
52 Z. Su, J. Fan, M. Chen, T.-a. Okamura and W.-Y. Sun, *Cryst. Growth Des.*, 2011, **11**, 1159-1169.
53 L. Luo, P. Wang, G.-C. Xu, Q. Liu, K. Chen, Y. Lu, Y. Zhao and W.-Y. Sun, *Cryst. Growth Des.*, 2012, **12**, 2634-2645.
54 X. Xu, X. Zhang, X. Liu, L. Wang and E. Wang, *CrystEngComm*, 2012, **14**, 3264-3270.
55 X.-H. Zhou, H.-H. Li and W. Huang, *Inorg. Chim. Acta*, 2012, **384**, 184-188.
56 S. Mistri, E. Zangrando, A. Figuerola, A. Adhikary, S. Konar, J. Cano and S. C. Manna, *Cryst. Growth Des.*, 2014, **14**, 3276-3285.
57 Q. Sun, Q. Yue, J.-Y. Zhang, L. Wang, X. Li and E.-Q. Gao, *Cryst. Growth Des.*, 2009, **9**, 2310-2317.
58 Q. Sun, Y.-Q. Wang, A.-L. Cheng, K. Wang and E.-Q. Gao, *Cryst. Growth Des.*, 2012, **12**, 2234-2241.
59 D. Liu, N.-Y. Li, F.-Z. Deng, Y.-F. Wang, Y. Xu, G.-Y. Xie and Z.-L. Zheng, *J. Mol. Struct.*, 2013, **1034**, 271-275.
60 Q. Sun, J.-Y. Zhang, H. Tian, Y.-Q. Wang and E.-Q. Gao, *Inorg. Chem. Commun.*, 2009, **12**, 426-429.
61 Y. Fukuda, S. Seto, H. Furuta, H. Ebisu, Y. Oomori and Terashima, *J. Med. Chem.*, 2001, **44**, 1396-1406.
62 G. M. Sheldrick, *SADABS, Program for Empirical Absorption Correction*, University of Göttingen, Göttingen, Germany, 1996.
63 G. M. Sheldrick., *SHELXTL*, Bruker Analytical X-ray Instruments Inc., Madison, Wisconsin, USA, 1998.
64 C.-B. Liu, L. Lu, Z.-L. Xu and Q.-W. Wang, *Acta Crystallogr., Sect. E: Struct. Rep. Online*, 2007, **63**, m2595.
65 M. O'Keeffe, M. A. Peskov, S. J. Ramsden and O. M. Yaghi, *Acc. Chem. Res.*, 2008, **41**, 1782-1789.
66 V. A. Blatov, *IUCr CompComm Newsletter*, 2006, **7**, 4. http://www.topos.ssu.samara.ru.

Graphic Abstract

The isomeric coordination polymers derived from *p*- and *m*-phenylenediacrylates contains similar homochiral motifs (hydrogen-bonded layers or μ-$O_{carboxylate}$ bridged helical chains**)**, but only the *m* ligand, with assistance of hydrogen bonds, induces spontaneous resolution to generate 3D homochiral networks.